Nuclear Physics B86 (1975) 125–141. North-Holland Publishing Company

COMPARISON OF EXCHANGE MECHANISMS IN $\pi N \to \rho N$ AND PION PHOTO- AND ELECTROPRODUCTION

A.C. IRVING *
Cern, Geneva

Received 23 September 1974
(Revised 5 November 1974)

Abstract: Rho-, photo- and electroproduction are compared and contrasted from a t-channel exchange point of view. A common exchange mechanism is evident. Systematic differences associated with the variable mass of the vector particle are found – in particular, the mass dependence of the non-pole-like contributions is reminiscent of that seen in higher mass resonance production. Naive vector meson dominance arguments which do not allow for these mass-dependent effects are shown to disagree both qualitatively and quantitatively with the data. We emphasize the implications of this, and similar studies, for an understanding of absorption effects in two-body scattering.

1. Introduction

Theoretical and phenomenological studies of small angle resonance production [1–6] from a t-channel exchange point of view have shown that exchange mechanisms can have a dependence on both the mass and the quantum numbers of external particles. The similar quantum numbers of the produced resonances in $\pi^- p \to (\rho^0, f^0, g^0)n$ allow the isolation of effects dependent on mass. The phenomenological decrease (with increasing mass) of the ratio of natural to unnatural pairty exchange [5, 7] is qualitatively described by dual theories, but a similar decrease in the ratio of cut (background) corrections to π exchange is not clearly understood. This decrease in the absorptive corrections is also present in the p-wave component of $\pi^- p \to \pi^+ \pi^- n$ when studied as a function of mass [5]. In this paper we investigate the evidence for the mass dependence of exchange mechanisms in ρ-production ($q^2 \equiv m_V^2 = m_\rho^2$), $\pi^\pm$ photoproduction ($q^2 = 0$) and $\pi^\pm$ electroproduction ($q^2 \lesssim 0$).

ρ-production data is simply described by a three-component exchange model [6, 8] viz. π and A_2 t-channel exchanges with s-channel cut corrections. Since the same quantum numbers are exchanged, charged pion photoproduction data may be analogously decomposed and the resulting components examined for mass de-

* Address from October 1974: Dept. of Applied Mathematics and Theoretical Physics, Liverpool University, UK.

pendence. We use data on both s- and t-dependence to disentangle the components. Although high-energy π-electroproduction data is as yet sparse, it provides important information on the q^2 dependence of exchange components.

The processes under consideration may be linked numerically by the vector dominance model (VDM) [9]. By a critical examination of the available data we isolate those features of the model's failure which are due to mass dependences in the exchange mechanism, and those which stem directly from the vector meson dominance assumption itself.

Sect. 2 contains a discussion of our model for vector production and the constraints due to gauge invariance. The salient features of the data and our interpretation of them, are presented in sect. 3. Concluding remarks are in sect. 4.

2. Model for vector production

We consider the process

$$\pi^- p \to \rho^o n, \tag{2.1}$$

$$\gamma N \to \pi N, \tag{2.2}$$

where (2.2) represents π^+ and π^- photo-(electro-)production processes averaged to remove the isoscalar-isovector interference contribution. Since the isoscalar part is expected to be negligible at small $-t$, we can assume (2.1) and (2.2) to be dominated by the same exchanges and being related by time-reversal, to have the same helicity structure. The basic model we use is already described in the literature [6]. We summarize briefly the formalism.

2.1. Helicity structure

Process (2.1) has as measurable combinations of (s-channel) helicity amplitudes

$$\begin{aligned}
\sigma_0 &= \rho_{00} d\sigma/dt = |P_0|^2 = |P^o_{++}|^2 + |P^o_{+-}|^2 , \\
\sigma_{1-} &= (\rho_{11} - \rho_{1-1}) d\sigma/dt = |P_-|^2 = |P^-_{++}|^2 + |P^-_{+-}|^2 , \\
\sigma_{1+} &= (\rho_{11} + \rho_{1-1}) d\sigma/dt = |P_+|^2 = |P^+_{++}|^2 + |P^+_{+-}|^2 , \\
\sqrt{2}\,\mathrm{Re}\,\rho_{10}\, d\sigma/dt &= \mathrm{Re}(P^-_{++} P^{o*}_{++} + P^-_{+-} P^{o*}_{+-}).
\end{aligned} \tag{2.3}$$

P^o and P^- (P^+) represent unnatural (natural) parity exchange asymptotically.

For (2.2) the most commonly quoted observables are

$$\sigma^{\parallel} = \sigma(1-\Sigma) = |P_-|^2, \quad \sigma^{\perp} = \sigma(1+\Sigma) = |P_+|^2 , \tag{2.4}$$

where

$$\sigma = \tfrac{1}{2}(\sigma^{\parallel} + \sigma^{\perp}) \tag{2.5}$$

is the unpolarized differential cross section and Σ the polarized photon asymmetry.

When the photon in (2.2) is virtual, i.e. in π electroproduction, the measurables are:

$$\begin{aligned} \bar{\sigma} &= (\rho_{11} + \epsilon\rho_{00})\,\mathrm{d}\sigma/\mathrm{d}t = \tfrac{1}{2}[\,|P_+|^2 + |P_-|^2] + \epsilon\,|P_0|^2\,, \\ \sigma_T &= -\rho_{1-1}\,\mathrm{d}\sigma/\mathrm{d}t = \tfrac{1}{2}[\,|P_-|^2 - |P_+|^2]\,, \\ \sigma_I &= \sqrt{2}\,\mathrm{Re}\,\rho_{10}\,\mathrm{d}\sigma/\mathrm{d}t = \mathrm{Re}[P^-_{++}P^{0*}_{++} + P^-_{+-}P^{0*}_{+-}]\,, \end{aligned} \tag{2.6}$$

where ϵ ($\leqslant 1$) is an experimentally known kinematical quantity.

2.2. Exchange model

Our exchange model may be summarized

$$\begin{aligned} P^0_{+-} &= \pi^0_{+-}\,, & P^0_{++} &= \pi^0_{+-}\sqrt{t_{\min}/t}\,, \\ P^-_{+-} &= \pi^-_{+-} + C\,, & P^-_{++} &= \pi^-_{+-}\sqrt{t_{\min}/t}\,, \\ P^+_{+-} &= A_{+-} + C\,, & P^+_{++} &= A_{++}\,, \end{aligned} \tag{2.7}$$

where π^0_{+-} is the dominant s-channel π Regge-pole exchange contribution parametrized exactly * as in ref. [6]:

$$\pi^0_{+-} \propto \frac{\sqrt{-t'}}{\mu^2 - t}\,|q|\,, \quad |q| = (m_V^2)^{\frac{1}{2}} = |q^2|^{\frac{1}{2}}\,. \tag{2.8}$$

C is a cut correction to the zero net helicity flip ($n = 0$) amplitude and A_{++} the A_2 exchange contributions, again parametrized as in ref. [6]. The ratio

$$\pi^-_{+-}/\pi^0_{+-} = 2\sqrt{-t'}/|q| \tag{2.9}$$

and the factor $|q|$ in eq. (2.8) are those suggested by the dual model [3, 6] which specifies the basic t-channel helicity 0 and 1 π-exchange residues. This is further discussed in the next paragraph.

2.3. Gauge invariance

It is well known that single π exchange in process (2.2)

* The nucleon non-flip π-exchange contributions P^0_{++}, P^-_{++} are included so as to give the correct small $-t$ behaviour at non-asymptotic energies.

$$\pi^{o}_{+-} \propto \frac{\sqrt{-t'}}{\mu^2 - t} \frac{q^2 + t - \mu^2}{|q|} ,$$
$$\pi^{-}_{+-}/\pi^{o}_{+-} = \frac{2\sqrt{-t'}\,|q|}{q^2 + t - \mu^2} , \tag{2.10}$$

does not by itself satisfy gauge invariance. A simple and economical means of assuring this to add nucleon exchange Born terms as in the electric Born term model [10, 11]

$$P^{o}_{+-} \propto \frac{\sqrt{-t'}}{\mu^2 - t} \frac{q^2 + t - \mu^2}{|q|} \left[1 - R(q^2) \frac{t - \mu^2}{q^2 + t - \mu^2}\right],$$
$$P^{-}_{+-} \propto \frac{1}{\mu^2 - t} \left[-2t' + R(q^2)(t - \mu^2)\right] , \tag{2.11}$$
$$P^{+}_{+-} \propto -R(q^2) ,$$

where $R(q^2) = F_1(q^2)/F_\pi(q^2)$ is the ratio of nucleon to pion form factors [11]. Since $R(0) = 1$, the gauge invariance condition

$$P^{o}_{+-} \sim |q| \tag{2.12}$$

is satisfied. This model satisfactorily describes many features of photo- and electroproduction data at small $-t$ and low energies.

A result formally identical to (2.11) (with $R(m_\rho^2) = 1$) is given by the Williams model of absorbed π exchange in vector production [12]. In this model, as with the gauge invariant Born term model, the gauge invariance mechanism in P^{o}_{+-} is closely correlated with that which yields the non-pole corrections (cut) in P^{-}_{+-}.

In the dual model prescription for Reggeized π exchange (egs. (2.8) and (2.9)), the additional t-channel helicity one coupling [3] is just such as to make the π (Regge) pole contribution gauge invariant by itself, leaving the cut correction C in P^{-}_{+-} essentially unconstrained. We note that these three approaches all imply a P^{o}_{+-} behaviour like (2.8) rather than (2.10), but we choose to use the dual model prescription because of its theoretical and phenomenological attractiveness [6]. In fact, the correction C deduced in phenomenological applications to ρ-production is very similar to the Williams prescription (2.11).

2.4. Direct channel and exchange models

Exchange models have enjoyed almost unrivalled success in describing resonance production processes above 3 GeV/c. To a large extent this is because duality ideas, so successful for $0^- \tfrac{1}{2}^+$ scattering processes, do not easily accommodate exchange of more than one naturality (as in $\pi^- p \to \rho^o n$). Furthermore, it is not possible to

build up the sharp t-structure of π exchange from a finite set of equivalent resonances. Any realistic s-channel resonance model must therefore add in some t-channel exchange and so suffers problems with possible double counting. The electric Born term model, if restricted to π and nucleon exchange diagrams, cannot describe the structure which is seen in $|P_+|^2$ for $|t| > 0.1$ GeV^2 and which is ascribed to A_2 exchange in a t-channel model.

We therefore consider it useful to extend the Regge t-channel description to include charged pion photoproduction and electroproduction, a domain hitherto dominated by the Born term class of models.

3. Mass-dependent effects in the data

The application of models like that of sect. 2 in ρ-production is well discussed in the literature [6, 8]. We briefly review the main features with reference to the sample data* shown in fig. 1 (helicity-one components only).

3.1. ρ-production ($q^2 = m_\rho^2$)

The helicity-zero π exchange contribution is fixed by the $|P_0|^2$ data. Knowing the π_-/π_0 ratio (e.g. eqs. (2.9)), the cut contribution C is fixed by a knowledge of $|P_-|^2$ and $\mathrm{Re}\,\rho_{10}$. Since phase coherence,

$$2(\mathrm{Re}\,\rho_{10})^2 (\mathrm{d}\sigma/\mathrm{d}t)^2 = |P_0|^2 |P_-|^2 \tag{3.1}$$

is approximately satisfied in ρ production [15], the measurable $\mathrm{Re}\,\rho_{10}$ yields little extra information (not shown in fig. 1). Finally, the C/A_2 exchange separation is made using $|P_+|^2$.

The dip in $|P_-|^2$ (zero in $\mathrm{Re}\,\rho_{10}$) at $-t \approx \mu^2$ is interpreted as a cancellation between C (dominant at small $-t$) and π_- (dominant at larger $-t$). This mechanism is exhibited in eqs. (2.11) which, for unnatural parity exchange, are equivalent to our model at small $-t$ [eqs. (2.7)]. The shoulder structure in $|P_+|^2$ near $-t \approx 0.2$ GeV^2 is interpreted as a similar interference between C and A_2 but a phase difference prevents the complete cancellation as seen in $|P_-|^2$. Confirmation of this interpretation is given by ρ–ω interference phase information and by the observed α_{eff} of $|P_+|^2$ [6].

3.2. Photoproduction ($q^2 = 0$)

The sample data shown in fig. 1 show great similarity with ρ production data at

* The ρ production (2.77 GeV/c [13, 14] and 17.2 GeV/c [15, 14]) and photoproduction data (3.4 GeV [16, 17] and 16 GeV [18]) have been linearly interpolated to obtain a common set of reference t-values. The energies were chosen such as to span a significant range and to facilitate comparison with available (low-energy) data on π electroproduction.

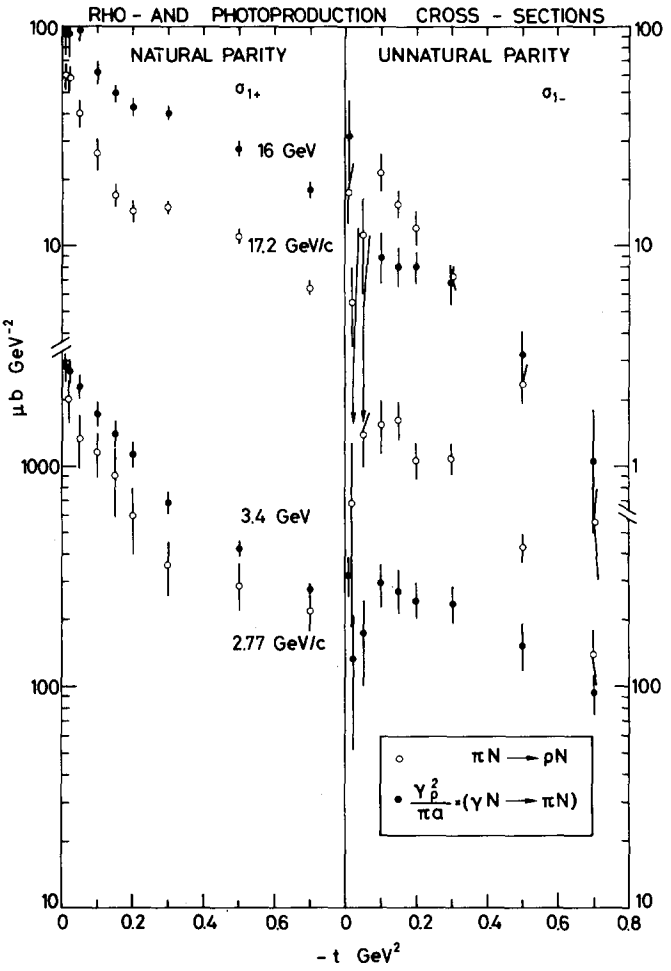

Fig. 1 The natural and unnatural parity exchange helicity-one (*s*-channel) cross sections for $\pi^- p \to \rho^0 n$ (at p_L = 2.77 [13], 17.2 [15] GeV/*c*) and $\gamma N \to \pi N$ (at E_γ = 3.4 [16, 17], 16 [18] GeV). As in all subsequent figures, the data is shown interpolated at standard *t*-values. To aid comparison, the photoproduction data (an average of π^+ and π^- photoproduction) has been multiplied by the VDM factor $\gamma_\rho^2/\pi\alpha$ ($\approx$ 350).

nearby energies. There is, of course, no helicity zero component at $q^2 = 0$ (gauge invariance) but the observables $|P_-|^2$ and $|P_+|^2$ have common features at $q^2 = m_\rho^2$ and $q^2 = 0$, viz. a forward spike and shoulder or dip at $t = -0.2$ GeV^2 in $|P_+|^2$; forward spike and deep dip at $-t \approx 0.02$ GeV^2 in $|P_-|^2$. Closer study shows [11, 16, 19], however, that the natural/unnatural parity ratio is significantly higher in the photon process. This emphasized in fig. 2 where we show

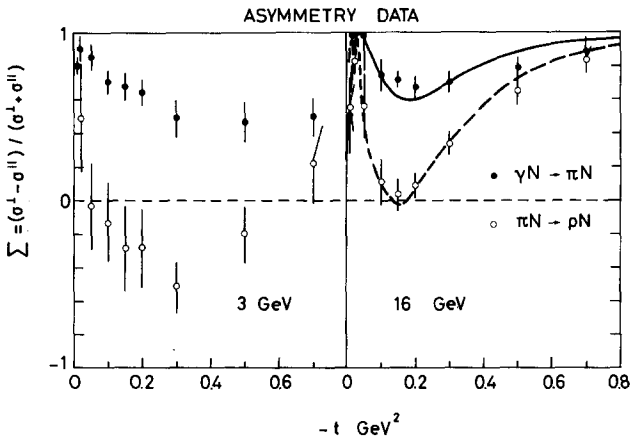

Fig. 2. A comparison of the polarized photoproduction asymmetry data, $\Sigma = (\sigma^{\perp} - \sigma^{\parallel})/(\sigma^{\perp} + \sigma^{\parallel})$, with the analogous data for $\pi^- p \to \rho^0 n$. Data sets in the neighbourhood of 3 and 16 GeV demonstrate the strong energy dependence of this quantity. The curves represent the fit of our model.

$$\Sigma = \frac{\sigma^{\perp} - \sigma^{\parallel}}{\sigma^{\perp} + \sigma^{\parallel}} = \frac{|P_+|^2 - |P_-|^2}{|P_+|^2 + |P_-|^2} = \frac{\rho_{1-1}}{\rho_{11}} \tag{3.2}$$

for $q^2 = m_\rho^2$ and $q^2 = 0$. It is clear that no single (q^2 independent) model such as the electric Born term model ‡ or Williams model can describe both of these.

In view of the discussion of the previous paragraphs, a probable explanation of this difference is that (at least for $|t| \leqslant 0.2$ GeV^2) the cut C is larger at $q^2 = 0$. The effect of this would be to cancel π more completely in $|P_-|^2$ so giving a smaller result for $|t| \geqslant 0.02$ GeV^2 and reduce the cancellation with A_2 in $|P_+|^2$ yielding a larger result for $|t| \lesssim 0.2$ GeV^2. At still larger $-t$, the possibility of an increased A_2 contribution at $q^2 = 0$ giving increased asymmetry Σ, is not excluded of course.

Further confirmation of the above exchange decomposition may be sought in a study of energy dependence. In ref. [6] it was shown how the rapid rise of $\alpha_{\text{eff}}(|P_+|^2)$ at $-t \approx 0.2$ GeV^2 is associated with the transition from $|C|^2$ to $\text{Re}(A_2 C^*)$ dominance of $|P_+|^2$. In fig. 3 this rise is exhibited by the quantity $\alpha_{\text{eff}}(|P_+|^2) - \alpha_{\text{eff}}(|P_-|)^2$ for $q^2 = m_\rho^2$ and $q^2 = 0$‡‡.

‡ This model is already known [9, 17] to inadequately describe the photoproduction asymmetry for $\sim t \geqslant 2\mu^2$. At smaller $-t$, since *any reasonable* strength of "cut" (or nucleon Born term) gives $\Sigma = 0$ at $t = 0$ followed by a very rapid rise with $-t$, the photoproduction data has never provided a stringent test of this model.

‡‡ We study the ratio $|P_+|^2/|P_-|^2$ to reduce the effects of normalization uncertainties in the data. $\alpha_{\text{eff}}(|P_-|^2)$ is expected to be similar in both cases [$\approx \alpha_\pi(t)$; $|t| \geqslant 0.1$ GeV^2].

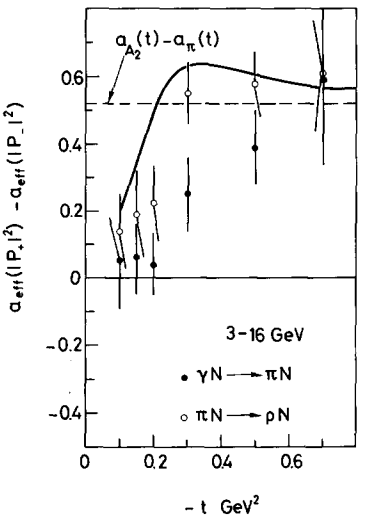

Fig. 3. The quantity $\alpha_{\text{eff}}(|P_+|^2) - \alpha_{\text{eff}}(|P_-|^2)$ for ρ and photoproduction calculated from the 3 and 16 GeV data sets. The dotted and solid curves, respectively, show the predictions of simple Regge pole exchange and of our ρ production model [6].

Also shown is our model prediction for $q^2 = m_\rho^2$. It is unclear to what extent quantitative information may be extracted from this comparison, since the corresponding quantity extracted from 6–17 GeV/c ρ production data (fig. 2 of ref. [6]), while qualitatively the same, lies higher than our model (not lower as here). Such a strong energy dependence between 3 and 6 GeV/c indicates that, while exchange mechanisms are already in evidence, 3 GeV is not a sufficiently asymptotic energy for a detailed study of effects crucially dependent on a Regge behaviour (e.g., a prediction of $|P_+|/|P_-|^2$). It is, however, to be expected that effects due to q^2 dependence of exchange components will nonetheless be observed whatever the energy. Fig. 2 shows this to be the case.

3.3. Electroproduction ($q^2 \lesssim 0$)

In π electroproduction $|P_+|^2$ and $|P_-|^2$ are not directly measurable (see eq. (2.6)). However, the crucial feature of our interpretation, the cut/π cancellation, is observable in $\sigma_I \equiv \sqrt{2}\,\text{Re}\,\rho_{10}\,d\sigma/dt$ just as for ρ production. If the deduced trend towards larger C/π_- found in going from $q^2 = m_\rho^2$ to $q^2 = 0$ were to continue for $q^2 < 0$, we expect the zero in σ_I to move out from $-t \approx 0.02$ GeV^2 towards larger $-t$ (see fig. 4(b)). This is what is observed in the data [20] shown in fig. 4(a).

The electric Born term model predicts [10] the position of the zero in σ_I to be essentially independent of q^2 (at $-t \approx \mu^2$) and so contradicts the data [20]. Likewise, simple vector dominance applied to $\pi^- p \to \rho^0 n$ data predicts the zero to be at $-t \approx \mu^2$ [21].

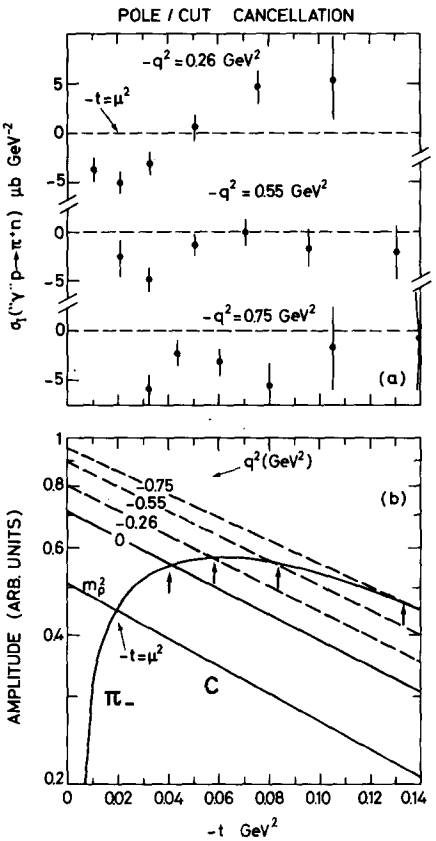

Fig. 4. (a) The longitudinal/transverse interference cross section $\sigma_I (\equiv \sqrt{2}\,\mathrm{Re}\,\rho_{10}\,\mathrm{d}\sigma/\mathrm{d}t)$ for π^+ electroproduction for $-q^2 = 0.26$, 0.55 and 0.75 GeV^2 [20]. (b) Model amplitude components (moduli shown) demonstrating the q^2 dependence of the cut C (eqs. (3.3) and (3.4) of the text) which is capable of explaining the $\rho-$, photo- and electroproduction data. The arrows indicate the zero position of P_- at each value of q^2 and may be directly compared with the zero observed in σ_I (part (a)).

If the phase-coherence condition (3.1) were well satisfied in the (rather low-energy) data, a complete decomposition into P_0, $P_\pm$ could be made. Unfortunately the low statistics of the data and inherently small $|P_-|^2$, do not allow this to be meaningfully performed. However, if $|P_-|^2$ is indeed small, as suggested by our model and the $q^2 = 0$ data for $|t| \gtrsim \mu^2$, eqs. (2.6) allow a separation of the dominant $|P_0|^2$ [20]. A comparison of $|P_0|^2$ at $q^2 = m_\rho^2$ and $q^2 < 0$ will be made in subsect. 3.6.

3.4. Quantitative model

An illuminating way to exhibit the difference between amplitudes at $q^2 = 0$ and

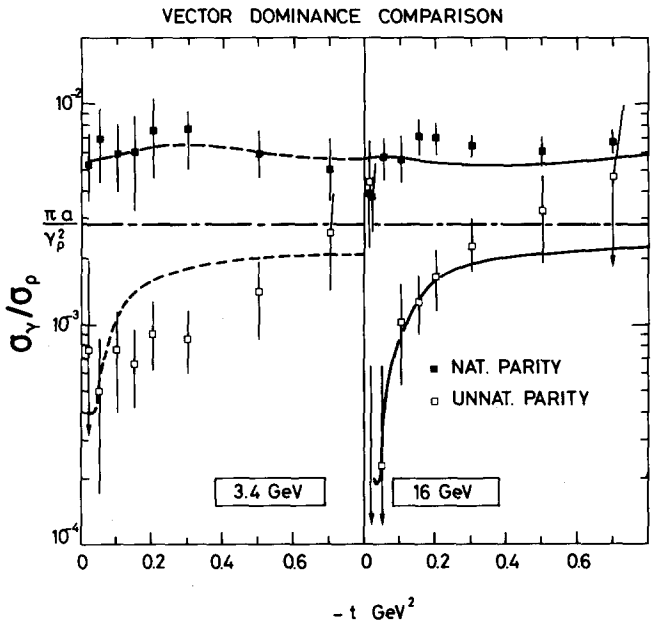

Fig. 5. The ratio of photoproduction to ρ-production cross sections scaled to a common energy (see text). The comparison is made for natural and unnatural parity exchange at 3 and 16 GeV. The model fit at 16 GeV (prediction at 3 GeV) is shown by a solid (dotted) curve. The chain-dotted line is the value expected from vector dominance.

$q^2 = m_\rho^2$ is to plot the ratio of photoproduction and ρ-production cross sections for natural and unnatural parity exchange. In fig. 5 we show these ratios at 3.4 and 16 GeV ‡. For comparison, a line has been drawn at the value suggested by naive vector dominance — 2.85×10^{-3} using $\gamma_\rho^2/4\pi = 0.64$ [22]. The changes in behaviour of $|P_+|^2$ and $|P_-|^2$ are clearly seen. With reference to the vector dominance line, the natural parity ratio is larger than expected, while for $0.02 < -t < 0.3$ the unnatural parity is much smaller. In a previous paragraph we explained how a cut increasing with $-q^2$ can account for this at $|t| \lesssim 0.2$ GeV^2. At larger $-t$, the vector dominance arguments are tenable for $|P_+|^2_\gamma/|P_+|^2_\rho$ only if A_2/π is also allowed to increase with $-q^2$.

Three uncertainties associated with VDM applications are often discussed.

(a) What value of $\gamma_\rho^2/4\pi$ should be used [23]? This problem in no way affects our arguments since the VDM violations seen in fig. 5 are typically 200% rather than 20% effects.

‡ The ρ data have been scaled ($\sim s^{-2}$) to the same c.m. energy as the corresponding γ data and have been normalized to include the resonance tails. Uncertainties in normalization prescription are, in effect, equivalent to redefining $\gamma_\rho^2/4\pi$ for the purposes of this work.

(b) In which helicity frame should the comparison be made [9]? We would argue that the similar small $-t$ structure seen in $|P_-|^2_\gamma$ and $|P_-|^2_\rho$ suggests the comparison is most favourably made in the s-channel. $|P_-|^2_\rho$ rapidly loses this structure when rotated to other frames.

(c) How important are higher mass vector mesons [24]? In the small q^2 region under discussion, only low mass ($\lesssim 1600$ MeV) mesons are expected to affect vector dominance calculations. In particular, since we are concerned mainly with π exchange and its associated cuts, the most important corrections would be from a low-mass ρ' vector meson decaying into 2π. The evidence for such a resonance is at best inconclusive [25]. Until mass, width, and branching ratios of suitable candidates are established, this question remains open.

The full curves in fig. 5 show the result of allowing the magnitude and slope of the cut, and magnitude of the A_2 contribution to vary as a function of q^2 while fitting the data for $\pi^- p \to \rho^0 n$ at 17.2 GeV/c and $\gamma N \to \pi N$ data at 16 GeV *. The broken curve gives a subsequent prediction for the corresponding 3.4 GeV ratios. For this fit the cut and A_2 magnitudes at $q^2 = 0$ were augmented by the factor 1.4 (compared with $q^2 = m_\rho^2$ [6]) and the cut t-dependence made flatter by $e^{0.5t}$. The t-dependence of the data (fig. 5) indicate that A_2/π and C/π increase approximately proportionately. For convenience we use the same factor for each.

Some comments on these results are in order.

(a) The ratio $|P_-|^2_\gamma/|P_-|^2_\rho$ is seen to tend to the vector dominance value for large $-t$ (> 0.5 GeV^2). In our model this is interpreted as being due to the dominance of $|P_-|^2$ by $|\pi_-|^2$ which is independent of q^2.

(b) The increase of the ratio A_2/π (with $-q^2$) is an effect which is seen in studies of higher mass resonance production [5, 7] where it may be understood in a dual theory approach [1–3].

(c) An increase of the ratio C/π is also found in production processes over a large range of q^2. Particularly relevant to the present study is the observation of this effect in P-wave $\pi^+\pi^-$ production from $q^2 = m^2_{\pi\pi} = 0.40$ to 0.85 GeV^2 [26].

(d) The maximum of the ratio $\sigma^\gamma_{1+}/\sigma^\rho_{1+}$ seen near $-t = 0.2$ is interpretable as being due to the flattening of the cut with $-q^2$.

Fig. 4(b) shows the π contribution to P_- together with the cut contributions determined (at $\sim$ 16 GeV) from the ρ and photon data. If we regard the σ_1 data of fig. 4(a)** as evidence of P_- possessing a zero in $-t$ at 0.05 GeV^2 for $q^2 = -0.26$ GeV^2, at 0.08 for $q^2 = -0.55$ GeV^2 and at 0.12 for $q^2 = -0.75$ GeV^2, we may deduce the mass dependence of the cut for spacelike q^2 to be approximately as shown by the dotted lines. A simple parametrization of the cut, which describes the observed behaviour between $q^2 = m_\rho^2$ and $q^2 = -0.75$ GeV^2 and is consistent with the (large) positive q^2 behaviour (c), is

* We apply VDM to our model amplitudes rather than to cross sections so that in practice the ratio of flux factors k^2_π/k^2_γ modifies multiplicatively the simple factor $\pi\alpha/\gamma^2_\rho$ discussed in the text.

** We do not expect isoscalar/isovector interference to alter this discussion of π^+ electroproduction data since it is restricted to small $-t$ (< 0.1 GeV^2) and concerns unnatural parity for which no appreciable interference is seen in photoproduction as discussed later.

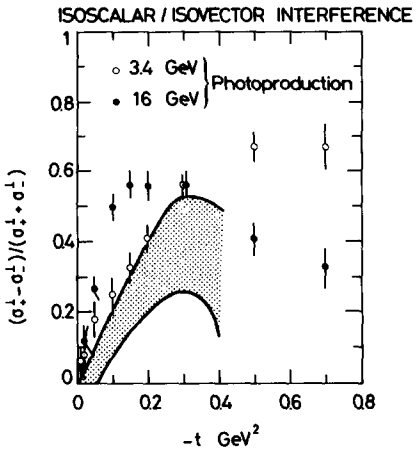

Fig. 6. The quantity $(\sigma_+^\perp - \sigma_-^\perp)/(\sigma_+^\perp + \sigma_-^\perp)$ measuring the isoscalar/isovector interference in charged π photoproduction at 3.4 [16, 17] and 16 [18] GeV. The shaded region represents the analogous quantity estimated from vector-meson production data [27] (see text).

$$C = g_c e^{b_c t} , \tag{3.3}$$

where

$$g_c(q^2)/g_c(m_\rho^2) = 1.40 + (q^2/m_\rho^2)(1-1.40),$$
$$b_c(q^2)/b_c(m_\rho^2) = 0.93 - (q^2/m_\rho^2)(1-0.93). \tag{3.4}$$

3.5. Isoscalar/isovector interference

The photoproduction processes $\gamma p \to \pi^+ n$ and $\gamma n \to \pi^- p$ have unequal cross sections (σ^+ and σ^-) in the presence of isoscalar/isovector interference. For example, simple VDM would predict

$$\sigma^+ \propto |\rho + \frac{1}{2.8}\omega|^2, \quad \sigma^- \propto |\rho - \frac{1}{2.8}\omega|^2, \tag{3.5}$$

where $\rho(\omega)$ represents the amplitude for $\pi^- p \to \rho^0 n(\omega^0 n)$. So far we have considered

$$\sigma \equiv \tfrac{1}{2}(\sigma^+ + \sigma^-) = |\rho|^2 + (1/2.8)^2|\omega|^2 \approx |\rho|^2 . \tag{3.6}$$

Although there is little evidence of $\sigma^+/\sigma^- \neq 1$ for unnatural parity exchange [16], the ratio $\sigma_\perp^+/\sigma_\perp^-$ is well known to grow appreciably above unity as $-t$ increases beyond 0.02 GeV^2 [16, 18]. In fig. 6 we show $(\sigma_\perp^+ - \sigma_\perp^-)/(\sigma_\perp^+ + \sigma_\perp^-)$ which in VDM language (eq. (3.5)) is

$$\frac{\sigma_\perp^+ - \sigma_\perp^-}{\sigma_\perp^+ + \sigma_\perp^-} = \frac{2(1/2.8)\,|\omega/\rho|\,\xi\cos\phi}{1+(1/2.8)^2|\omega/\rho|^2} \approx \frac{1}{2.8}\cdot 2\left|\frac{\omega}{\rho}\right|\xi\cos\phi\,. \tag{3.7}$$

ξ and ϕ [6] are, respectively, the coherence and phase angle between the natural parity ρ and ω amplitudes. For comparison we show the bounds on the analogous interference quantity extracted ‡ from $K^- p \to K^{*0} n$ and $K^+ n \to K^{*0} p$ data at 4 GeV [27], viz.

$$\frac{1}{2.8}\,\frac{\sigma_{1+}(\bar{K}N) - \sigma_{1+}(KN)}{\sigma_{1+}(\bar{K}N) + \sigma_{1+}(KN)}\,x \approx \frac{1}{2.8}\cdot 2\left|\frac{\omega}{\rho}\right|\xi\cos\phi\,, \tag{3.8}$$

where

$$x = \frac{1+|\omega/\rho|^2}{1+(1/2.8)^2|\omega/\rho|^2} \tag{3.9}$$

is a correction factor which allows for non-negligible contributions from $|\omega/\rho|^2$. It is seen that the observed isoscalar/isovector interference is larger than expected at 4 GeV. The effect is largest at large $-t$. Since in this region the interference term is certainly not smaller at $q^2 = 0$ than at $q^2 = m_\rho^2$ (assuming vector dominance) one may conjecture that the ρ exchange contribution to ω production increases at least as fast with $-q^2$ as does A_2 exchange in ρ production.

3.6. Helicity-zero components

Gauge invariance demands that $|P_0|^2$ in electroproduction vanish as q^2 when $q^2 \to 0$. Apart from this, the only q^2 dependence which VDM predicts in electroproduction cross section is that due to the ρ meson propagator [11]:

$$\frac{\sigma_\gamma(q^2)}{\sigma_\rho(m_\rho^2)} = \left(\frac{m_\rho^2}{m_\rho^2 - q^2}\right)^2 \frac{\pi\alpha}{\gamma_\rho^2}\,. \tag{3.10}$$

In fig. 7 we show the quantity $\hat{\sigma}_0^\gamma/\sigma_0^\rho$ which is the ratio of helicity-zero cross sections with the VDM factor (3.10) divided out. It is plotted, as a function of q^2 at two t-values. One notices that (a) there is a residual q^2 dependence roughly consistent with the gauge invariance factor $|q^2|/m_\rho^2$ and (b) the electroproduction data [20] are rather larger than VDM expectation. Point (b) might be regarded as evidence for the necessity to include higher mass vector mesons in vector dominance

‡ The K^*, ρ and ω production data for natural parity exchange is in accord with SU(3) symmetry expectation [27].

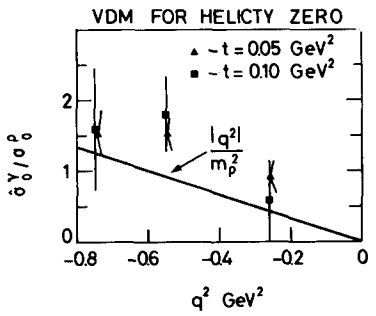

Fig. 7. The ratio of π^+ electroproduction and ρ production helicity zero components. To aid comparison with VDM, the factor $(m_\rho^2/(m_\rho^2-q^2))^2 \pi\alpha/\gamma\rho^2$ (see eq. (3.10) of text) has been divided out and the data scaled by s^{-2} to a common energy. Also shown is the gauge invariance expectation (at small q^2) for this quantity $(|q|^2/m_\rho^2)$.

comparisons at appreciable values of $|q|^2$. As regards exchange mechanisms, we do not anticipate sstrong mass-dependent effects in $|P_0|/|q|$ itself — our model attributes it to pure pion exchange.

Higher statistics charged pion electroproduction data would enable a detailed amplitude analysis to be made (see subsect. 3.3). Further progress could then be made in studying the validity of the widely used vector meson dominance hypothesis, and also in finding the connection (if any) between the mass-dependent effects noted here and those seen in resonance production processes.

3.7. Origin of q^2 dependent absorption effects

We have shown that it is meaningful to describe ρ, photo- and electroproduction at small $-t$ in terms of π exchange (well behaved as a function of q^2) and a cut correction $C(q^2)$ which increases systematically as q^2 varies from $+m_\rho^2$ to $-m_\rho^2$. Little is known theoretically concerning the precise dynamical origin of the cut corrections observed in two-body scattering. One intuitively appealing approach is to ascribe them to s-channel absorptive effects and to calculate them as a convolution of the pole-exchange amplitude and the corresponding elastic amplitude. Such calculations are known to give only qualitatively correct results and are certainly wrong in details [8].

In real or virtual π photoproduction the relevant diffractive amplitude could be taken as that of ρ electroproduction — final state absorption due to πN elastic scattering would lead to no extra q^2 dependence. A general result of such absorption models is that the cut at $t = 0$ is given by

$$C \propto \frac{A}{B},$$

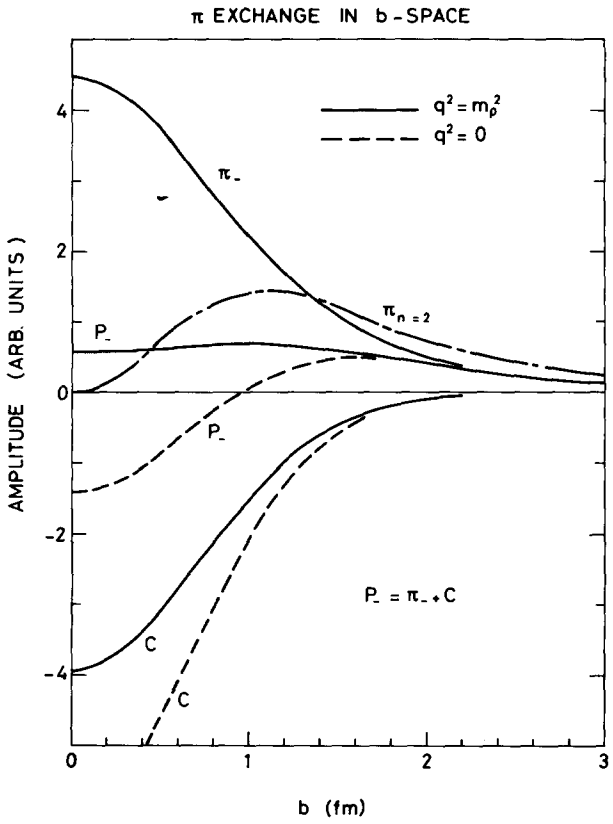

Fig. 8. The impact parameter transforms ($\int\sqrt{-t'}\,d\sqrt{-t'}J_n(b\sqrt{-t'})f_n(t)$) of the amplitude components of $P_-(q^2)$ which are shown in fig. 4(b). Solid (dotted) curves show the values at $q^2 = m_\rho^2(0)$. Also shown is the b transform of the double helicity flip ($n = 2$) component of π exchange.

where A is the diffractive amplitude at $t = 0$ and B its slope in t. While there is experimental [28] and theoretical [29] evidence that $B(q^2)$ probably decreases with $-q^2$, $A(q^2)$ is certainly a more strongly decreasing function of $-q^2$ [30]. Any overall increase in $C(q^2)$ would therefore have to come from considering the coupling of other intermediate inelastic states (high mass vector mesons) as a function of q^2. A quantitative absorption model for these effects is not feasible.

In impact parameter (b) space, the amplitude P_- manifests considerable absorption at small b as compared to the π-pole contribution itself. Fig. 8 shows the components* $\pi_-(b)$, $C(b)$ and their resultant $P_-(b)$ at $q^2 = m_\rho^2$ and $q^2 = 0$. As

* These are b-space transforms of the t-space quantities of fig. 4(b). Note that $\pi_-(b)$ and $P_-(b)$ contain (unequal) contributions from both net helicity flips, $n = 0$ *and* 2. $P_-(b)$ shows a maximum near $b = 1$ fermi in analogy with what is known of $n = 0$ vector exchange amplitudes [31]. The $n = 0$ component of $P_-(b)$ does not.

$C(q^2)$ becomes stronger and flatter in t-space, the degree of absorption increases and extends to larger b. Unfortunately, quantitative discussion of the amplitudes at small b would require knowledge of the large $-t$ behaviour, in particular the cut slope. Nonetheless the qualitative remarks made here are independent of our precise model for the t-dependences. Unabsorbed π exchange, π_-, gives a large central (small b) component in b space, while $\pi_0(b)$ is already peripheral (maximum around 1 fm). It therefore seems the case that the interaction becomes more peripheral as the vector particle becomes progressively lighter.

The photon-hadron interactions are known to become increasingly point-like at large $-q^2$. Deep inelastic phenomena bear witness to this. By "increasingly point-like" we mean that the collison no longer resembles that between extensive hadrons which both have structure. It is therefore reasonable to suppose that absorptive phenomena in two-body scattering which depend on the hadronic nature of the colliding objects will reflect this transition from a hadron-like photon (at $q^2 \approx m_\rho^2$), to a point-like photon at large space-like q^2.

4. Conclusions

We have demonstrated the value of examining ρ, photo- and electroproduction from a common t-channel point of view. The following observations are made.

(a) ρ production ($q^2 = m_\rho^2$), photoproduction ($q^2 = 0$), electroproduction ($q^2 \leqslant 0$) data give evidence of a common t-channel exchange mechanism – π, A_2 pole exchange with s-channel absorption.

(b) There is direct experimental evidence for a strong q^2 dependence of the absorption corrections (cuts) required to fit the data. The cuts apparently increase with $-q^2$, an effect previously noted in higher mass resonance production ($q^2 \equiv m_{\pi\pi}^2$).

(c) If the vector dominance model (VDM) is to be valid for the natural parity exchange amplitudes, the ratio A_2/π must be an increasing function of $-q^2$. This increase is also observed in higher mass resonance production and qualitatively understood in dual theories.

(d) The observed isoscalar/isovector interference in natural parity exchange π photoproduction is larger than expected (through VDM) from ρ and ω vector meson production.

(e) The helicity-zero cross section in π electroproduction is significantly larger than expected from ρ production via gauge invariance and VDM.

(f) VDM applied without due regard to mass-dependent effects in the exchange mechanism has been shown to give qualitatively and quantitatively incorrect results.

(g) The increase of absorption with $-q^2$ is conjectured to be related to the transition of the photon from hadron- to point-like behaviour. Whether this effect, in fact, is associated with the special properties of the photon or is a more general geometrical attribute of hadrons is of considerable importance in an understanding of two-body interactions.

We thank Chris Michael for his active interest and encouragement at all stage of this work.

References

[1] P. Hoyer, R.G. Roberts and D.P. Roy, Nucl. Phys. B56 (1973) 173.
[2] P. Hoyer and J. Kwiencinski, Nucl. Phys. B60 (1973) 26;
P. Hoyer, P. Estabrooks and A.D. Martin, Phys. Rev. D10 (1974) 80.
[3] C. Michael, Nucl. Phys. B63 (1973) 431.
[4] W. Ochs and F. Wagner, Phys. Letters 44B (1973) 271.
[5] A.D. Martin, Proc. 4th Int. Symp. on multiparticle hadrodynamics, ed. F. Duimo et al. (Pavia, 1973) p. 203.
[6] A.C. Irving and C. Michael, Nucl. Phys. B82 (1974) 282.
[7] B. Hyams et al., Phys. Letters 51B (1974) 272.
[8] R.D. Field and D.P. Sidhu, Phys. Rev. D10 (1974) 89.
[9] J.J. Sakurai, Proc. 4th Int. Symp. on electron and photon interactions at high energies, Liverpool, 1969, p. 91 and references therein.
[10] F.A. Berends and R. Gastmans, Phys. Rev. D5 (1972) 204.
[11] R.W. Manweiler and W. Schmidt, Phys. Rev. D3 (1971) 2752; Phys. Rev. Letters 33B (1970) 366.
[12] P.K. Williams, Phys. Rev. D1 (1970) 1312.
[13] J. Baton et al., Nucl. Phys. B21 (1970) 551; B45 (1972) 205.
[14] P. Estabrooks and A.D. Martin, Phys. Letters 42B (1972) 229.
[15] G. Grayer et al., Nucl. Phys. B75 (1974) 189.
[16] H. Burfeindt et al., Nucl. Phys. B59 (1973) 87.
[17] H. Burfeindt et al., Phys. Letters 33B (1970) 509;
P. Heide et al., Phys. Rev. Letters 21 (1968) 248.
[18] D.J. Sherden et al., Phys. Rev. Letters 30 (1973) 1230.
[19] C. Michael, Invited talk at the 17th Int. Conf. on high-energy physics, London (1974).
[20] C. Driver et al., Phys. Letters 35B (1971) 77, 81.
[21] F.A. Berends and R. Gastmans, Phys. Rev. Letters 27 (1971) 124;
H. Fraas and D. Schildknecht, Phys. Letters 35B (1971) 72.
[22] J. Lefrançois, Proc. Int. Symp. on electron and photon interactions at high energy, Cornell, 1971, p.60.
[23] S.J. Brodsky, F.E. Close and J.F. Gunion, Phys. Rev. D6 (1972) 177.
[24] H. Fraas, B.J. Read and S. Schildknecht, DESY preprint 74-23 (1974).
[25] Particle Data Group, Phys. Letters 50B (1974) 1.
[26] P. Estabrooks and A.D. Martin, Nucl. Phys. B79 (1974) 301.
[27] A.B. Wicklund et al., Argonne National Laboratory preprint (1974).
[28] R. Talman, Proc. 4th Int. Symp. on electron and photon interactions at high energies, Bonn, 1973, ed. H. Rollnik and W. Pfeil, (North-Holland, Amsterdam, 1974) p. 145.
[29] J.D. Bjorken, Proc. 11th Session of the Scottish Universities' Summer School in Physics, 1970 (Academic Press, London, 1971) p. 516.
[30] L. Ahrens et al., Phys. Rev. D9 (1974) 1894.
[31] F. Halzen and C. Michael, Phys. Letters 36B (1971) 367;
M. Davier and H. Harari, Phys. Letters 35B (1971) 239;
A.C. Irving, A.D. Martin and V. Barger, Nuovo Cimento 16A (1973) 573.